Chapter 1
Crystallographic Aspects of Interfaces in Ferroelectrics and Related Materials

Experimental studies of single crystals (SCs) of polar dielectrics show that, in an external electric field E, these materials can exhibit either linear or non-linear behaviour [1, 2]. A non-linear dependence of the polarization P on E in a certain range of E is observed, for instance, in ferroelectric (FE) and antiferroelectric SCs [1,3,4], poled ceramics and SCs of FE solid solutions [3,4], and composites based on FE ceramics [5]. The presence of FE and ferroelastic domains (or mechanical twins), heterophase regions, and fluctuations of composition makes the $P(E)$ dependence complicated and is caused by many physical and crystallographic factors that are studied in the last decades [1, 3, 4]. Moreover, the dependence of physical properties on the domain structure (DS) in FE SCs and ceramic grains represents an independent problem that is solved by means of experimental and theoretical methods [6–8]. An interest in the aforementioned subjects stems from a necessity to study an important link between the domain configurations and physical properties of FEs, to consider the role of the domain-orientation processes in forming the physical properties, to describe their anomalies in heterophase states on mesoscopic and macroscopic levels, and to predict ways for the formation and rearrangement of DS at the structural phase transitions. To solve these and related problems, it is important to understand the physical phenomena that are concerned with the presence of both DS and heterophase states in FEs. One of the main links in the interpretation of the physical phenomena in polydomain and/or heterophase FE SCs is the interfaces [9] that represent systems of boundaries between the domains (or domain regions) and boundaries between the phases (they can be split into domains). It should be added that the polydomain SC as a model object plays the leading role in the hierarchy of the physical properties 'single-domain FE SC – polydomain FE SC – FE polycrystal – poled FE ceramic – composite based on FE ceramic', and an important example of this hierarchy was first analysed for FEs of the $PbTiO_3$ type [7, 8, 10].

Chapter 1 is devoted to the analysis of some important results in the study and classification of various interfaces that are observed in polydomain and heterophase FE SCs and related materials. An emphasis is placed on crystallographic methods

V. Yu. Topolov, *Heterogeneous Ferroelectric Solid Solutions*,
Springer Series in Materials Science 151, DOI 10.1007/978-3-642-22483-6_1,

[9] that are applied to study complicated DSs and their rearrangement, heterophase states, features of the formation of the new phase, etc., in FE solid solutions.

1.1 Domain Structures and Interfaces Between Polydomain Regions

1.1.1 Formation of Domain Structures in Ferroelectric Single Crystals

Below the temperature of the FE phase transition many SCs are split into domains or regions with different orientations of the spontaneous polarization vector $\boldsymbol{P_s}$ [1–3]. The FE domains are also regarded as macroscopic regions wherein the unit cells have parallel orientations of the spontaneous dipole moments at $E = 0$. An aggregate of the domains divided by the interfaces (domain walls, boundaries between the domain regions, etc.) constitutes DS observed and described in experimental works (see, e.g., monographs [1–4, 11–13]). Analogous regions corresponding to certain orientations of the spontaneous polarization vectors of the sublattices $\pm\boldsymbol{P_a}$ are observed in antiferroelectric SCs [2, 3, 13]. The regions with different tensors of spontaneous strains in an initial coordinate system form ferroelastic SCs that are often regarded as mechanical analogues of Fes [12].

The first principal propositions on a correlation between the orientation of the FE domains, domain walls, and macrosymmetry of the physical properties of the SC sample were formulated by Zheludev and Shuvalov [14–19]. In the absence of external influences, such as electric or mechanical fields, the appearance of the FE domains is equally probable along each of the crystallographically equivalent directions that are regarded as polar axes. FE SCs are traditionally divided into two groups in accordance with the number of polar axes [2, 3, 11, 13]. The first group contains electrically uniaxial SCs that are divided only into the 180° domains with antiparallel spontaneous polarization directions, $+\boldsymbol{P_s}$ and $-\boldsymbol{P_s}$. The second group represents electrically multiaxial SCs with non-180° domains oriented along the crystallographically equivalent directions in the FE phase. In the second group, the 180° domains are present side by side with the non-180° domains. The number of permissible orientations of the spontaneous polarization vectors is $n = N_1/N_2$, where N_1 and N_2 are orders of the point symmetry group of the prototype phase and the domain (twin component), respectively. If all the possible domain types are present in the SC sample in equal volume fractions, then this sample is characterized by the same point symmetry group as in the prototype phase [2, 13, 18, 19]. However, not all the domain types can be observed in real SCs [11, 13] because of an influence of crystal-growth conditions, phase-transition kinetics, external fields, etc.

Changes in energy of the system at the structural phase transition are main reasons for the domain formation in FE SCs. According to results [1–3, 11], the reason for 180°-domain formation is jump of the depolarizing field at the first-order

phase transition, and the reason for non-180°-domain formation is the jump of the spontaneous strains of the SC unit cell. Both the jumps are caused by a change in the spontaneous polarization $\boldsymbol{P_s}$ at the phase transition. In a case of the paraelectric-FE first-order phase transition, the jump of $\boldsymbol{P_s}$ (from 0 to a certain value) takes place at Curie temperature T_C. Various 180° domain patterns are formed under the influence of an internal electric field and by screening of the spontaneous polarization by free charge carriers in the SC sample [11]. The domain-formation processes lead to a minimization of an electric contribution to the free energy of the SC sample [20]. The electric contribution comprises the volume energy of the depolarizing field of the sample as a whole and the surface energy of domain walls or domain boundaries therein.

Theoretical concepts on domain walls and the formation of DSs [21] at the first-order phase transition are based on the determination of the effective free energy as a function of the polarization field. This approach is useful, for example, at the description of the effect of the elastic strain on the non-180° DS that takes place, for example, in the tetragonal phase of perovskite-type FEs ($BaTiO_3$, $PbTiO_3$, $KNbO_3$, etc.) and related solid solutions. The free energy of FE SC depends on inhomogeneous regions, such as domain walls and modulated structures. Based on the thermodynamic study of the free energy of FE, Cao [22] analysed inhomogeneous microstructures in the FE phase of solid solutions of $(Pb_{1-3x/2}La_x)TiO_3$. In a certain x range, these inhomogeneous microstructures represent spatial amplitude modulations inside domains of this system, and the development of the modulated structure is caused by La dopants. A time evolution of the 90° DS in FE was predicted in work [23]. As follows from results [23], the elastic long-range interactions between the polarization fields lead to a lamellar 90° DS (mechanical twins) and frozen domain patterns which are observed in a series of FE SCs. The model proposed in paper [24] enables one to describe the lamellar or spiked morphology of the 180° domains in FE SCs by taking into account the electrostatic interaction. The model concept [24] is applied for a prediction of trends in the formation (or subsequent rearrangement) of the DS in the presence of the external electric field.

Experimental results on the formation of 180° and 90° DSs in the tetragonal phase of multiaxial FE SCs of the perovskite type at the first-order phase transition were generalized by Fesenko et al. [11]. According to experimental data, the FE phase in $BaTiO_3$ SCs is split into both the 180° and 90° domains near the Curie temperature $T_C = 393\,K$. The corresponding DS being formed in the $BaTiO_3$ SC sample, wherein a planar interphase boundary moves at the paraelectric–FE phase transition, remains almost unchanged on cooling down to room temperature. Rules in the formation of the DS are formulated [11] with due regard for jumps of the depolarizing field, spontaneous strains, and entropy at the first-order phase transition. These jumps are caused by the jump of the spontaneous polarization $\boldsymbol{P_s}(T_C)$. Based on numerous experimental results, Fesenko et al. proposed a classification of domain patterns [11] affected by the jumps of the physical parameters in multiaxial FE SCs. In this classification, some interconnections between the jumps are taken into account. In addition to the electric and elastic fields that are directly concerned

with complex DSs in multiaxial FE SCs, the latent heat also influences [11] phase-transition kinetics, the motion of the interphase boundary [25] over the SC sample, and the formation of the DS.

Taking into consideration numerous experimental results on polydomain (twinned) FE SCs [1–4, 11, 25], one can mention the following factors that actively influence the formation of the DS: electrostatic energy of the depolarizing field of SC, electric conductivity of SC at the phase transition, elastic energy concerned with the phase coexistence and defects, surface energy of domain wall (boundaries), anisotropy of the physical properties, the simultaneous formation of a number of nuclei of the new phase, external electric and/or elastic fields, temperature gradient over the SC sample, and cooling rate of this sample undergoing the FE phase transition. Examples of the quantitative description of the influence of the separate factors on the formation of the 180° and non-180° DSs are present in monographs [1–3, 11].

1.1.2 Elastic-Matching Concept and Its Application to Domain Boundaries

The elastic interaction between the phases in SCs [26] and between the domains in the FE phase plays an important role in the formation of DS [11, 25] with various planar, wedge-shaped, zigzag, or diffused interfaces. The domains that are observed near these interfaces are mainly non-180° and promote minimization of an elastic contribution into the free energy of the SC sample. In contrast to the traditional 180° (FE) domains, these domains are often called elastic domains [26] or twins [11]. Moreover, aggregates of the plane-parallel twins form a polysynthetic twin (polytwin), and the polysynthetic twin can be a part of a more complicated hierarchical structure (so-called polysandwich structure) in SC. As noted by Roytburd [26], the polysandwich structure is characteristic of many phase-transition types in solids, for instance, martensitic, ferroelastic, ordering, diffusion, and decomposition types. The polysandwich structure can be present in SCs that undergo both the first-order and second-order phase transitions. Decreasing the elastic energy at the formation of the new phase in solids can be concerned with the integration of DSs or, in other words, with the formation of hierarchical DSs. Hereby the polytwins serve as individual domains and form DSs of the second order, third order, etc. [26].

The study of the formation of DS in FE SCs is often carried out in terms of crystallographic [9, 27] and thermodynamic [26, 28, 29] theories. Lowering the energy of the internal mechanical stress field associated with the phase coexistence leads to the certain (preferable) orientation of the nucleus of the new phase or the interphase boundary and to the formation of equilibrium DSs. Theoretical studies [28] show that the plate-like shape of the nucleus of the new phase provides the maximum localization of the elastic field at the structural phase transition. The equilibrium DS is one of the milestones in the interpretation of experimental data on phase transitions of the martensitic type [11, 25], that is, the first-order phase

transitions going through a coherent heterophase state [29] at the jump in unit-cell strains. According to the idea developed in work [30–32], the new polydomain phase retains its contact with the parent phase and, consequently, the interphase boundary must be undistorted (or unstrained) *on average*. This boundary, being one of the interfaces studied in solids, is called zero-net-strain plane (ZNSP) [9, 27], invariant plane [26], plane of the zero averaged distortion [30,31], or stress free. The zero-averaged distortion means that averaging the elements of distortion matrices is carried out over a macroscopic volume that involves a large number of domains within a specific phase.

Authors of papers [29–31] considered important examples of the martensitic phase transitions in metals and alloys. A reconstruction of the crystal structure at these phase transitions is associated with a strain field that gives rise to changes in the shape of the sample, and atomic displacements therein are less than the unit-cell parameters. While this transformation does not need a diffusion of atoms at a large distance, the martensitic phase transition is often regarded as diffusionless. The twins appearing at the martensitic phase transition are regarded rather as elastic domains [26] than as a result of deformation twinning of the martensitic phase. In the last decades, the phase transitions of the martensistic type were studied not only in metals and alloys, but also in molecular SCs, ferroelastics, Fes, and antiferroelectrics [11]. Examples of the application of the concepts of the martensitic phase transition to the FE phase transition in perovskite-type SCs are given in monograph [11]. The martensitic phase transitions that lead to polydomain structures with the non-zero elastic energy (i.e., without the formation of ZNSPs) were studied in terms of thermodynamics [29].

The presence of the interphase boundary that obey conditions for ZNSPs at the first-order phase transition means that the excessive elastic energy concerned with the jumps of the unit-cell parameters of SC vanishes in the heterophase state. It is also assumed that the interphase boundary remains coherent at the phase transformation [32, 33]. As noted by Larché [33], the concept of coherency is crystallographic in nature. Lowering the elastic energy and, as a consequence, the minimization of the free energy of the heterophase system undergoing the structural phase transition may be concerned with loss of coherency and twinning. In case of loss of coherency, systems of dislocations and cracks [33] can arise in solids to give rise to the considerable stress relief at the phase transition.

The crystallographic description of the interphase boundary at the first-order phase transition was proposed in a series of papers (see, e.g., [30, 31]). According to results [30, 31], the ZNSP with an optimal orientation arises from conditions for the complete stress relief in the two-phase SC sample. Vanishing the elastic energy means that the new phase (with lower symmetry) is split into domains of two types, and these domains are mechanical twin components. Optimal volume fractions of the domain types are determined in terms of the unit-cell parameters of the coexisting phases [30, 31] or in terms of spontaneous strains [11, 27] of the low-symmetry phase. The further mathematical modification of the crystallographic method by means of transformation distortion matrices was made by many authors, for example, Bilby and Christian [32] and Boulesteix et al. [34]. The infinitesimal

deformation approach and simple analytical solutions for interphase boundaries [35] make the crystallographic method more attractive for analysis of relationships between the parent and product phases in solids.

The problem of the existence of a planar unstrained interphase boundary between a prototype paraelastic phase and a ferroelastic phase was solved in work [34]. Based on this solution, Boulesteix et al. determined all possible orientations of the interphase boundaries in the analytical form. The general solution is realized [34] for phase transitions without a change in the unit-cell volume. Among 30 variants of the symmetry changes at the ferroelastic phase transitions in SCs, one can choose eight variants that correspond to exact solutions suitable for determination of the interphase-boundary orientations. In other cases the planar interphase boundary would appear at certain restrictions on the spontaneous strain tensor components. Results of the theoretical study are experimentally corroborated for a sequence of phase transitions in ferroelastic SCs [34, 36]. We note that the approach developed in papers [34, 36] can be effectively applied for the crystallographic interpretation of the interfaces in FE SCs.

The crystallographic method for the description of the two-phase SCs and formation of domains was developed in a series of papers (see, e.g., [37–42]). The allowable domain walls are determined to be walls that do not create long-range electric and elastic fields in FE SCs [37]. The absence of elastic fields is also required for domain walls that arise in the antiferroelectric and ferroelastic SCs [40]. This general requirement will be one of the principal conditions at the consideration of different interfaces in our monograph.

Permissible domain-wall orientations and possible types of corresponding walls related to all FE species were first determined by Fousek and Janovec [37–39]. It is assumed that in the FE species, the polarization is the order parameter of the phase transition. In an infinite and perfect FE SC, the condition for elastic matching between two domains with spontaneous polarization vectors $\boldsymbol{P}_s'$ and $\boldsymbol{P}_s'$ along the domain wall requires that the length of an elementary vector $\boldsymbol{ds}(ds_1,\ ds_2,\ ds_3)$ remains unchanged when crossing the domain wall. It means that the components of the vector $\boldsymbol{ds}$ obey condition [37]

$$hds_1 + kds_2 + lds_3 = 0, \tag{1.1}$$

where (hkl) are Miller indices of the unstrained domain wall. Equation (1.1) can be written in terms of the physical properties of the adjacent domains with $\boldsymbol{P}_s'$ and $\boldsymbol{P}_s'$ as follows:

$$\sum_{k,l=1}^{3} \Delta_{kl} ds_k ds_l = 0, \tag{1.2}$$

where the coefficients Δ_{kl} from (1.2) are given by

$$\Delta_{kl} = \sum_{i=1}^{3} g_{ikl} \left(P_i' - P_i''\right) + \sum_{i,j=1}^{3} Q_{ijkl} \left(P_i'' P_j'' - P_i' P_j'\right). \tag{1.3}$$

In (1.3) the piezoelectric coefficients g_{ikl} link the mechanical strain and electric displacement [2, 3] in the single-domain state and Q_{ijkl} are electrostrictive coefficients that link the mechanical strain and squared polarization [2] of the single-domain SC. Fousek and Janovec [37] described the FE domain walls of W_∞- and W_f-types with arbitrary (∞) and fixed (f) orientations, and a few kinds of the S-type walls that can be observed in polydomain FE SCs. The S-type domain walls have orientations [37] depending on directions of $\boldsymbol{P}_s'$ and $\boldsymbol{P}_s'$, values of g_{ikl} and/or Q_{ijkl} from (1.3). Tables of allowed orientations for the domain walls in all crystallographic species of SCs are given in paper [37].

The determination of the permissible domain walls and their orientations in ferroelastic SCs is carried out using (1.1) and (1.2) and condition [40]

$$\det \left|\left|\Delta_{kl}'\right|\right| = 0, \tag{1.4}$$

where $\Delta_{kl}' = S_{kl}' - S_{kl}''$ is the difference between the tensor components of the spontaneous strains S_{kl}' and S_{kl}'' in the unit cells that belong to the adjacent domains (twin components). The tensor components S_{kl}' and S_{kl}'' correspond to the coordinate axes of the prototype phase of the SC sample. Taking into account (1.4) and symmetry features of the domains, Sapriel determined the following types of the permissible planar domain walls [40]: W-walls with invariable orientations and W'-walls with orientations depending on the relative values of S_{kl}' and S_{kl}''. It should be added that the methods [37–40, 43] for determination of the domain-wall orientations were successfully used to characterize the forbidden domain boundaries in ferroelastic SCs [42] due to the significant influence of the elastic field therein.

Besides the domain-wall types described above, we mention the walls that are sometimes called antiphase boundaries or 360° domain walls. They arise as a result of elastic matching of two domain pairs with the 180° orientation of the spontaneous polarization vectors and with different tensors of spontaneous strains in separate domains. Some examples of these domain walls were observed in SCs exhibiting the FE and ferroelastic properties (see, e.g., papers [44–46]).

The description of the domain walls and complex DS-containing intersections of the domain (twin) walls, triple junctions, and irregular interfaces was carried out by Salje [47] in terms of dislocation densities. According to this concept, a possible break of the lattice planes in the domain (twin) walls is described as a continuous contribution of dislocations in ferroelastic and co-elastic SCs. The intersecting domain walls obey the condition for minimum of the wall energy. Differences in the domain-pattern formations were interpreted [48–52] at the study of elastic interactions in SCs at the structural phase transitions. The atomically coherent domain boundary obeys compatibility relations [40] (i.e., principles formulated by Sapriel) for components of the spontaneous strain tensor or the distortion tensor. However, the real domain conjunction in SCs spreads the anisotropic lattice distortion over some region around the domain boundary [49] with a fine 'tweed texture'[40, 50] (or tweed microstructure [51]) of lamellar domains, even in the case of the unstrained domain boundary. The presence of the tweed texture is consistent with the concept [26] of higher-order DSs in solids. The results of experimental

and theoretical studies of tweed microstructures in ferroelastic and co-elastic SCs are discussed in papers [50, 51]. Systems of cross-hatched tweed-like domains in FE phases were studied by Viehland et al. [53] in SCs of solid solutions of $(1 - x)Pb(Mg_{1/3}Nb_{2/3})O_3 - xPbTiO_3$ (PMN-xPT) with compositions near the morphotropic phase boundary (MPB). The PMN–xPT SCs are of great research interest due to the remarkable electromechanical and FE properties and complicated DS in heterophase states [53–57]. As follows from the experimental study [53], the domain self-organization is driven by the elastic compatibility, and the change between the miniature cross-hatched domains and the fine well-aligned striation domains also satisfies conditions for the elastic compatibility in the heterophase system.

1.1.3 Classification of Domain Boundaries in Ferroelectric Single Crystals

Besides the domain boundaries considered in Sect. 1.1.2, one can find other interesting examples of the domain boundaries described in experimental studies. The domain boundaries observed in FE SCs are classified [9] using a series of criteria (Fig. 1.1).

In the present review, we did not consider in detail some exotic situations concerned, for instance, with the formation of the non-coherent domain boundaries or even single-domain states [58] at the FE phase transition. As follows from results [58], the heterophase system comprising the single-domain FE phase also promotes a decrease of the elastic contribution into the free energy of the system, but conditions for the complete stress relief [30, 31] at the interphase boundary cannot be satisfied due to peculiarities of jumps of the unit-cell parameters at the phase transition. This behaviour is observed in FE-ferroelastic $Gd_2(MoO_4)_3$ SCs where the single-domain phase appears [59] at the FE phase transition. An analysis of the elastic-energy contribution caused by the phase coexistence enabled one to find the preferable orientation [58] of the crystallographic axes in the single-domain phase of $Gd_2(MoO_4)_3$. Finally, the effect of clamping the domain boundary in SCs leads to the appearance of irregularly shaped domains whose sizes are generally larger than those in the tweed microstructures [48].

1.1.4 Crystallographic Interpretation of Interfaces in the Case of Complicated Domain Structures

Metrat [60] developed the crystallographic theory [30–32] to describe the complex DS and its transformation at the first-order phase transition in FE SCs. The solution [60] allows the determination of the mutual orientation of the interface and the DS within one of the phase in the case of elastic matching of two polydomain phases

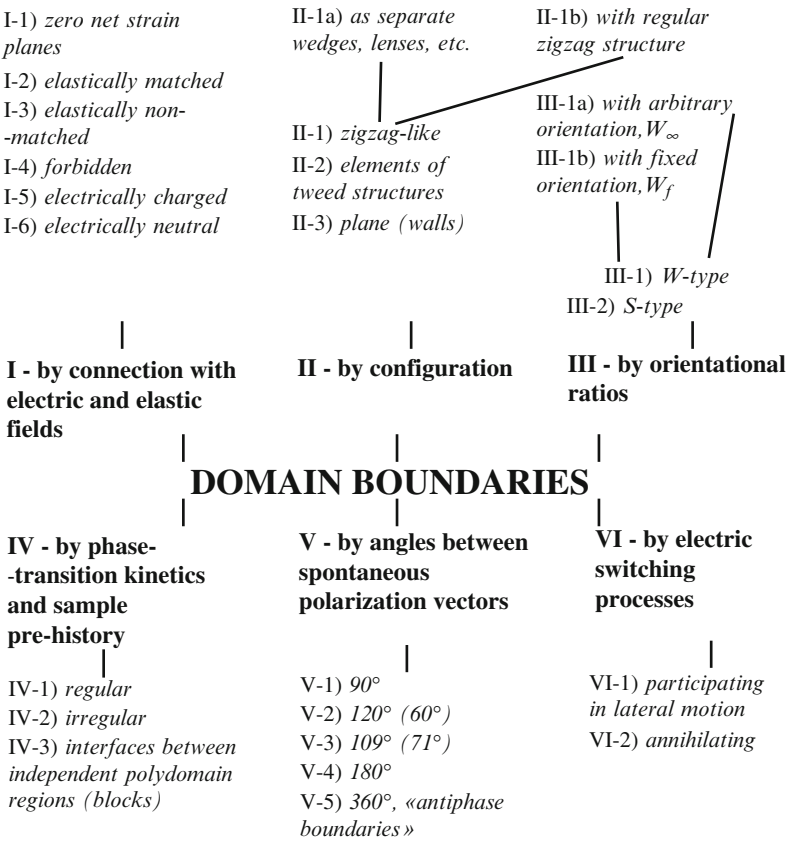

Fig. 1.1 Classification of domain boundaries observed in FE SCs (reprinted from paper by Topolov [9], with permission from Taylor and Francis)

or domain regions. It should be mentioned that 'interface' in this context means either *the interphase boundary* separating the coexisting phases or *the domain boundary* separating the domain regions of some polydomain (twinned) phase. A mathematical description of elastic matching of the coexisting phases (or domain regions) along the interface in FE or related SCs is based on the crystallographic concept [60].

According to Metrat [60], the coexisting polydomain phases (or domain regions) are characterized by the distortion matrices $||M_{ij}||$ and $||N_{ij}||$ that are expressed in terms of distortions of several domain types, their volume fractions, and angles of mutual rotation [30, 31] of the crystallographic axes of the adjacent domains. In contrast to the assumptions used in (1.2)–(1.4), conditions for the complete stress relief and the formation of the ZNSP along the interface are written in the more strict form:

$$\det \left|\left| D_{ij} \right|\right| = 0, \tag{1.5}$$

and

$$(D'_{ij})^2 \geq 0, \tag{1.6}$$

where elements of the $||D_{ij}||$ matrix (3×3) from (1.5) are given by

$$D_{ij} = \sum_{k=1}^{3} (N_{ik} N_{jk} - M_{ik} M_{jk}), \tag{1.7}$$

N_{ik} and M_{ik} are taken from the aforementioned distortion matrices, and $(D_{ij}{}')^2 = D_{ij}{}^2 - D_{ii} D_{jj}$ ($ij = 12$ and 13). Metrat [60] takes into account the second powers of the distortions of the adjacent phases or domain regions [see (1.7)]. It leads to complicated non-linear relationships between the volume fractions of the domains in the coexisting phases. The necessary conditions for the existence of the ZNSP [30, 31] are generalized and given by inequality (1.6). Based on the matrix elements D_{ij} from (1.7), one can determine the Miller indices (hkl) of the planar unstrained interfaces [60] as follows:

$$h_{1,2} = D_{11/} D_{1,2}, k_{1,2} = \left(D_{12} \pm D'_{12}\right) / D_{1,2} \text{ and } l_{1,2} = \left(D_{13} \pm D'_{13}\right) / D_{1,2}, \tag{1.8}$$

where $D_{1,2} = \left[D_{11}^2 + (D_{12} \pm D'_{12})^2 + (D_{13} \pm D'_{12})^2\right]^{1/2}$ is written in terms of D_{ij} and $D_{ij}{}'$ from (1.7) and (1.6), respectively. The possibility of application of conditions (1.5)–(1.8) for description of the polydomain (twinned) and heterophase SCs demonstrates obvious advantages of the Metrat's algorithm [60] in comparison to methods [30–32, 35, 37–40] proposed earlier. A comparative analysis of the crystallographic methods and some examples of calculations of characteristics of heterophase SCs are considered in Appendix A.

The Metrat's algorithm [60] and the matrix approach were applied to FEs and antiferroelectrics of different structural types for interpretation of experimental data on heavily twinned SCs, structural phase transitions, formation and rearrangement of DS, and features of phase coexistence at changes in temperature, molar concentration, or external stress (see, e.g., papers [27, 58, 61–64]). The matrix approach is also helpful in studying a connection between the elastic interaction of the phases and the behaviour of their unit-cell parameters in wide temperature or molar-concentration ranges [61, 64]. Based on experimental data and the Metrat's algorithm, Balyunis et al. [65] first characterized four types of the S-type boundaries in heavily twinned $PbZrO_3$ SCs and generalized the concepts by Fousek and Janovec [37] for a case of four twin components in the FE phase. Analytical conditions determining the thermal stability of the orientation of the S-type boundary studied in work [65] may be applied to various FE (antiferroelectric) perovskite-type SCs with complex DS or systems of twin components. Furthermore, it is possible to determine the unit-cell parameters more exactly using data from optical studies and crystal geometry of domain (twinned) regions with the S-type domain boundary whose orientation remains stable in a certain temperature range. This possibility was first

demonstrated at the determination of the temperature dependence of the shear angle ω of the perovskite unit cell in the antiferroelectric *Pbam* phase of $PbZrO_3$ SC [66].

The crystallographic study of the S-type boundaries [65, 66] in perovskite-type FE and antiferroelectric SCs revealed a difference between the orientation relations from the Metrat's algorithm (1.8) and the formulae derived from work by Fousek and Janovec [37]. In a case of elastic matching of the 60° domains (Fig. 1.2) in the orthorhombic phase of such SCs as $KNbO_3$, the distortion matrices of domains 1 and 2 are

$$\left|\left|M_{ij}\right|\right| = \begin{pmatrix} \eta_a & 0 & \eta \\ 0 & \eta_b & 0 \\ \eta & 0 & \eta_c \end{pmatrix} \quad \text{and} \quad \left|\left|N_{ij}\right|\right| = \begin{pmatrix} \eta_b & 0 & 0 \\ 0 & \eta_a & \eta \\ 0 & \eta & \eta_a \end{pmatrix}, \tag{1.9}$$

respectively, where η_a, η_b, and η are distortions of the perovskite unit cell along the a-, b-directions and in the (ac)-plane, respectively. The distortions from (1.9) can be written in terms of the spontaneous strains ξ_a^s, ξ_b^s and ξ^s of the perovskite unit cell as follows: $\eta_a = 1+\xi_a^s$, $\eta_b = 1+\xi_b^s$ and $\eta = 1+\xi^s$. Based on (1.5)–(1.9), we conclude that the following orientations of normal vectors to the unstrained domain wall are possible: $\boldsymbol{n}_1(1\bar{1}0)$ and $\boldsymbol{n}_2(hhl)$. The normal vector $\boldsymbol{n}_2$ characterizes the orientation of the S wall [27, 67]. In accordance with (1.8), components of the $\boldsymbol{n}_2$ vector are linked by the ratio

$$(l/h)_M = 4\eta\eta_a/(\eta_a^2 - \eta_b^2 + \eta^2). \tag{1.10}$$

The similar ratio of the Miller indices determined in terms of work [37] is expressed as follows:

$$(l/h)_{FJ} = 2\eta/(\eta_a - \eta_b). \tag{1.11}$$

Comparing the l/h ratios from (1.10) and (1.11), one can state that $\kappa = (l/h)_{FJ}/(l/h)_M \neq 1$ in the general case. As follows from evaluations [67] based on experimental values of the unit-cell parameters, κ equals 0.996 ($BaTiO_3$ SC at temperature $T = 277$ K), 0.995 ($PbHfO_3$ SC at $T = 298$ K), or 0.998 ($KNbO_3$ SC at $T = 298$ K) [67]. The difference $1 - \kappa$ increases with increasing the difference $\eta_a - \eta_b$ (i.e., as the difference of the unit-cell parameters a–b increases) under condition that $\eta^2 << \eta_a - \eta_b$. Data on the thermal stability of the orientation of the S wall in $PbZrO_3$ SC (see Appendix A) suggest that the inequality $0.99 < \kappa < 1$ is

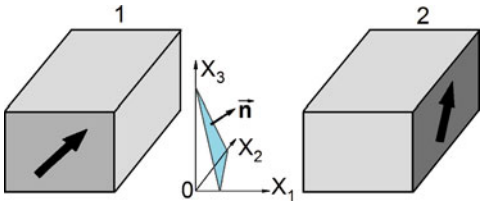

Fig. 1.2 Schematic arrangement of domains in the orthorhombic phase of perovskite-type FE SCs. Spontaneous polarization vectors of domains 1 and 2 are shown by arrows. $(X_1X_2X_3)$ is the rectangular coordinate system with axes parallel to the perovskite unit-cell axes in the cubic phase, $\boldsymbol{n}$ is the normal vector to the domain wall

valid in the wide temperature range. The reason for $\kappa \neq 1$ lies in the choice of basic conditions [38,60] for elastic matching of the adjacent domains [see (1.3) and (1.7)]. It is pertinent to add that (1.10) was applied for the more precise determination of the temperature dependence of the shear angle $\omega(T)$ of the perovskite unit cell in $PbZrO_3$ SC [66].

The approach developed in papers [65, 66] was applied to the S-type domain boundaries with various temperature dependences of the normal vector $\boldsymbol{n}_2(hhl)$ in orthorhombic $Pb(Zr_{1-x}Sn_x)O_3$ SCs. In papers [65, 66] the S-type boundaries play the role of interfaces separating the regions with 90° DS, and four non-180° domain types are involved in the crystallographic description of elastic matching of the domain regions. This crystallographic approach was also useful to interpret the non-monotonic temperature dependence of the S-type boundary orientation in two orthorhombic phases of $Pb(Yb_{0.5}Nb_{0.5})O_3$ SCs [68] and to show a link between the $\boldsymbol{n}_2(hhl)$ orientation and the unit-cell behaviour in a wide temperature range.

1.2 Phase Coexistence at First-Order Phase Transitions

1.2.1 Elastic Matching of Phases and Zero-Net-Strain Planes

The overwhelming majority of structural phase transitions in FE materials belong to the first-order transitions [1–4, 11]. They are accompanied by jumps of the unit-cell parameters, formation and growth of new-phase nuclei, motions of interphase boundaries, appearance or rearrangement of DS, and other physical phenomena. In every case, the transition of the system into a new stable state proceeds through a metastable state, and the system represents a heterogeneous (heterophase) medium wherein two [11, 61, 62, 69] or even three [63, 70] phases can coexist. These phases can be split into domains (mechanical twins) according to conditions [9, 27, 60] for the effective stress relief in the heterophase medium.

Below the Curie temperature, many FEs and related materials undergo structural phase transitions or a series of phase transitions between phases with different symmetry and DS [1–4]. Some results of determination of characteristics of the interphase boundaries and DS [71] within the framework of the Metrat's algorithm [60] are shown in Table 1.1. It is assumed that elastic matching of the coexisting phases and the full screening of electric fields of bond charges at surfaces of nuclei of the new phase take place. This screening promotes a lowering of the energy of the depolarizing field in the SC sample [11]. The domains (twin components) shown in Figs. 1.3–1.5 are separated by unstrained domain (twin) walls in accordance with the concept [37, 38]. Table 1.1 comprises data on the interphase boundaries at the following first-order phase transitions: paraelectric–FE, paraelectric–antiferroelectric, and FE–FE. In Figs. 1.3–1.5, each polydomain (twinned) phase contains the minimum number of the FE domain types (or twin components in the antiferroelectric state) at which the complete stress relief can be attained.

Table 1.1 Interphase boundaries and DSs which obey conditions (1.5) and (1.6) for ZNSPs in perovskite-type SCs

Point symmetry groups of coexisting phases	Domain types and volume fractions	Optimal orientations (hkl)[a] (or φ_{opt}) of interphase boundaries and optimal volume fractions of domains [71]
$m3m$ and $4mm$	Fig. 1.3	$BaTiO_3$: (506) ($\varphi_{opt} = 40.15°$) and $m_{opt} = 0.706$ $KNbO_3$: (405) ($\varphi_{opt} = 37.95°$) and $m_{opt} = 0.725$ $PbTiO_3$: (203) ($\varphi_{opt} = 33.76°$) and $m_{opt} = 0.764$
$m3m$ and 222	Fig. 1.4	$PbHfO_3$: (025) ($\varphi_{opt} = 68.03°$) and $m_{opt} = 0.877$
$4mm$ and $mm2$	Fig. 1.5a	$BaTiO_3$: (010) and $q_{opt} = 0.548$, $x_{opt} = 0.500$, and $y_{opt} = 0.259$
$4mm$ and $3m$	Fig. 1.5b	$Pb(Zr_{1-x}Ti_x)O_3$ near the MPB: the optimal orientation[b] is close to (010) at $t_{opt} = 0.294 - 0.554$
$4mm$ and $4mm$	Fig. 1.5c	$PbTiO_3$: the orientation changes from (708) at $m \to 0$ to (627) at $m \to 1$, the optimal volume fraction is $q_{opt} = A_{2,3} + B_{2,3}m$, where $A_2 = 0.0315$ and $B_2 = 0.953$, or $A_3 = 0.0143$ and $B_2 = 0.995$

[a] Miller indices (hkl) are determined with respect to the perovskite unit-cell axes in the cubic phase

[b] The spontaneous polarization vector in the single-domain $3m$ phase (Fig. 1.5b) can be oriented along a body diagonal of the perovskite unit cell, i.e., directions [111], $[\bar{1}11]$, $[1\bar{1}1]$, etc. are equivalent, and conditions for ZNSPs are fulfilled at the phase coexistence. The orientation of the spontaneous polarization vector in the $3m$ phase slightly influences the optimal volume fraction t_{opt} only

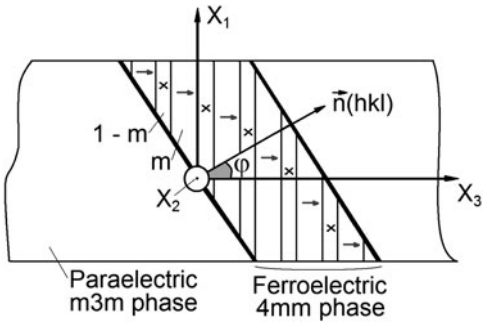

Fig. 1.3 Schematic arrangement of the lamellar nucleus (polydomain FE phase) in the paraelectric matrix. Directions of the spontaneous polarization vectors of 90° domains in the $4mm$ phase are shown by arrows (volume fraction m) and crosses (volume fraction $1 - m$). $\boldsymbol{n}$ is the normal vector to the interphase boundary and $\varphi = (\boldsymbol{n}, \widehat{} OX_3)$ is the angle of the orientation of the interphase boundary. Coordinate axes OX_j are parallel to the perovskite unit-cell axes in the cubic phase

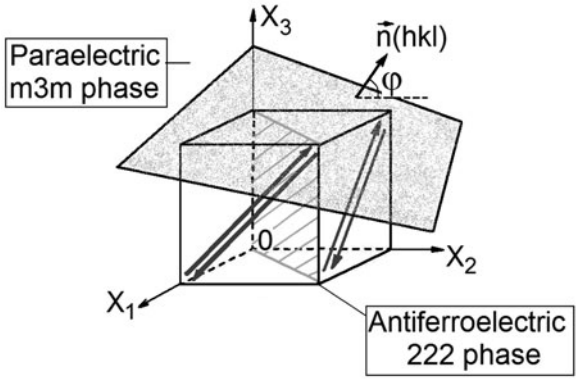

Fig. 1.4 Schematic arrangement of 60° twin components in the antiferroelectric 222 phase at the $m3m$ – 222 phase transition. Directions of the spontaneous antipolarization vectors are shown by arrows, m and $1 - m$ are volume fractions of the domains. $\boldsymbol{n}$ is the normal vector to the interphase boundary and $\varphi = (\boldsymbol{n}, \widehat{} \, OX_2)$ is the angle of the orientation of the interphase boundary. Coordinate axes OX_j are parallel to the perovskite unit-cell axes in the cubic phase

The majority of quantitative results from Table 1.1 are in good agreement with experimental data (see, e.g., [11, 69]). Metrat's algorithm [60] and the matrix approach for description of complex DSs promoted studying a connection between the elastic interaction in heterophase (polydomain) states and the behaviour of the unit-cell parameters in FE, antiferroelectric, and ferroelastic SCs. This behaviour is concerned with the necessary conditions [72] for the existence of the ZNSP at elastic matching of two polydomain phases. The necessary conditions introduced for the interphase boundaries at the cubic–tetragonal and cubic–orthorhombic phase transitions [30, 31] were generalized for the phase transitions between two polydomain phases of either tetragonal or orthorhombic symmetry. Based on the generalized necessary conditions, Topolov [72] formulated a series of selection rules to analyse experimental relations between the unit-cell distortions of the coexisting polydomain phases in perovskite-type FEs. These relations show that possibilities for the formation of the interphase boundary obeying conditions for ZNSP are more favourable at the FE–FE, FE–antiferroelectric, and antiferroelectric–antiferroelectric phase transitions than at the transitions between the FE (or antiferroelectric) and paraelectric phases. The polydomain phase with anisotropic spontaneous strains that strongly depend on the volume fraction and orientation of the non-180° domains provides additional 'degrees of freedom' for the stress relief in the heterophase structure wherein a few domain types (mechanical twin components) are present. We write 'degrees of freedom' in a figurative sense to avoid an analogy with a moving mechanical system.

A similar conclusion can be formulated on the basis of results [73] on the crystallographic description of the DS rearrangement and ZNSPs at the sequence of the first-order phase transitions $m3m - 4mm - mm2 - 3m$ in $BaTiO_3$ SC. It should

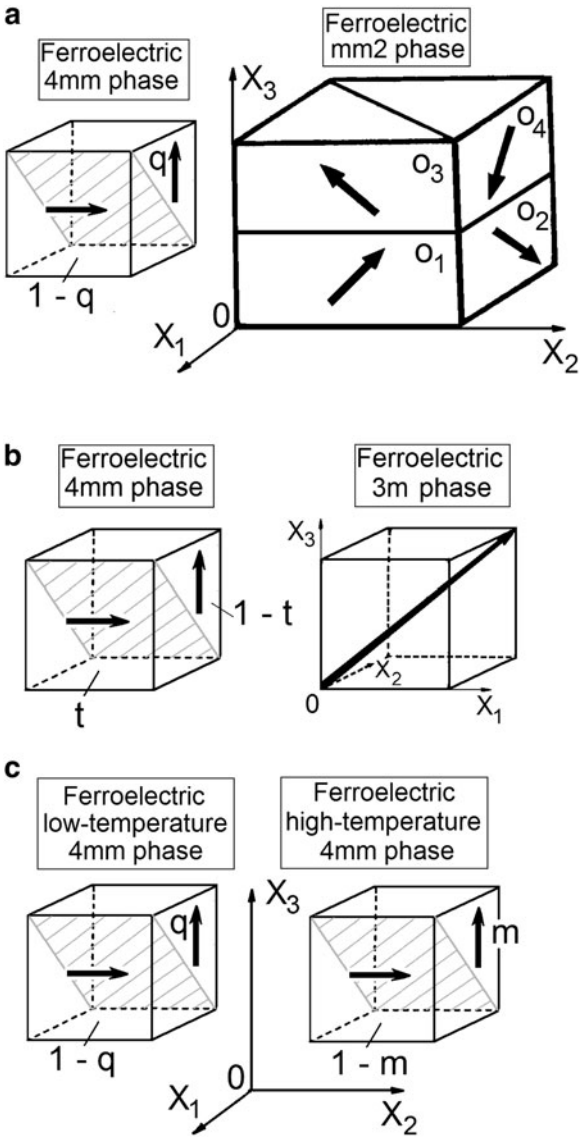

Fig. 1.5 Examples of the schematic arrangement of non-180° domains in the coexisting FE phases: (**a**) $4mm - mm2$, (**b**) $4mm - 3m$, and (**c**) $4mm - 4mm$. Spontaneous polarization vectors are shown by arrows. Coordinate axes OX_j are parallel to the perovskite unit-cell axes in the cubic phase. In schematic (a) q and $1 - q$ are volume fractions of the domains in the $4mm$ phase, and o_1, o_2, o_3, and o_4 are volume fractions of the domains in the $mm2$ phase. The volume fractions o_i are linked by parameters x and y as follows: $x = o_3 + o_4$ and $y = o_2 + o_4$. In schematic (**b**) t and $1 - t$ are volume fractions of the domains in the $4mm$ phase. In schematic (**c**) q and $1 - q$ are volume fractions of the domains in the low-temperature $4mm$ phase, m and $1 - m$ are volume fractions of the domains in the high-temperature $4mm$ phase

be added that paper [73] is the first publication where the Metrat's algorithm [60] was applied to the whole sequence of the phase transitions in polydomain FE SCs.

An unexpected issue is brought up at the study of the FE phase transition $m3m - 4mm$ in $K(Ta_{0.65}Nb_{0.35})O_3$ SC. Following the algorithm [60], one can obtain $\varphi_{opt} = 40.42°$ and $m_{opt} = 0.704$ at the phase coexistence (Fig. 1.3), so that the interphase boundary is oriented close to (506) in the perovskite axes. At the same time, the experimental study of the phase transition in $K(Ta_{0.65}Nb_{0.35})O_3$ SC [11] shows that the FE $4mm$ phase remains single domain, but its plate-like nucleus is parallel to (506). To the best of our knowledge, such behaviour has no analogues among FE SCs undergoing the first-order phase transition. The reason for the single-domain FE phase [71] lies in a small elastic energy of the single-domain nucleus in comparison with the energy that might be accumulated in the 90° domain walls after splitting this nucleus into the domains with the optimal volume fraction $m = m_{opt}$ (Fig. 1.3). Such a peculiarity takes place in the solid solution as the molar concentration of $KTaO_3$ approaches the value at which the first-order phase transition becomes the second-order one. According to data [11], $P_s(T_C) = 0.05\,C/m^2$ in this SC is about four times less than that in $BaTiO_3$ SC at the FE phase transition $m3m - 4mm$ and 8.4 times less than $P_s(T_C)$ in $PbTiO_3$ SC. Moreover, spontaneous strains of the perovskite unit cell of $K(Ta_{0.65}Nb_{0.35})O_3$ SC are oneto two orders of magnitude less than in $BaTiO_3$ SC and two orders of magnitude less than in $PbTiO_3$ SC.

Peculiarities of the elastic interaction between the polydomain phases of the FE nature have been studied in the last decades (see, e.g., papers [60, 69–72]). As follows from this study, the crystallographic description of elastic matching of the phases (domain regions) in terms of the Metrat's algorithm [60] is not exhaustive and should be supplemented by the thermodynamic theory of FEs [3, 11, 71, 74] and by the elasticity theory of anisotropic media [75, 76].

1.2.2 Stress Relief and Conical Interphase Boundaries

In Sect. 1.2.1, we did not mention possibilities of the stress relief at the cubic–rhombohedral phase transition. The first-order phase transition between the paraelectric cubic and FE rhombohedral phases is observed, for example, in SCs of $PbZrO_3$ [77], $Pb(Mg_{1/3}Nb_{2/3})O_3$ (PMN) under the external electric field [62], PMN–xPT [78], etc. The first attempt to provide a crystallographic interpretation of the interphase boundaries at the cubic–rhombohedral phase transition was made in work on $PbZrO_3$ SC [77]. Its rhombohedral ($R3m$) phase remains stable in the narrow temperature range (about 10 K) only. As is known from experimental data [77], the interphase boundaries in $PbZrO_3$ SCs have a complicated conical shape with a variable curvature radius, and the more complicated configuration of the boundary is observed near small domains of the rhombohedral phase. Moreover, virtually straight parts of the interphase boundary are observed when moving away from the domain wall. At the same time, changes in the non-180° DS of the

rhombohedral phase are insignificant and would not considerably influence the orientation and shape of the moving interphase boundary.

In the crystallographic study [77] of the cubic–rhombohedral phase transition in $PbZrO_3$ SC, the shape of the interphase boundary is approximated by a second-degree surface. This surface is described in the rectangular coordinate system $(X_1X_2X_3)$ as follows:

$$\sum_{i,j=1}^{3} D_{ij}\, x_i\, x_j = 0, \tag{1.12}$$

where the elements D_{ij} are expressed in terms of distortions of the coexisting phases [see (1.7)]. The rhombohedral phase is assumed to be split into 71° (109°) domains with the fixed orientations and variable volume fractions [77]. The surfaces are classified taking into account signs of the following invariants of (1.12):

$$I = D_{11} + D_{22} + D_{33},\ D = \det\left|\left|D_{ij}\right|\right| \text{ and}$$
$$J = \begin{vmatrix} D_{11} & D_{12} \\ D_{21} & D_{22} \end{vmatrix} + \begin{vmatrix} D_{22} & D_{23} \\ D_{32} & D_{33} \end{vmatrix} + \begin{vmatrix} D_{33} & D_{31} \\ D_{13} & D_{11} \end{vmatrix}. \tag{1.13}$$

Conical surfaces obey one of the following pairs of inequalities:

$$DI < 0 \text{ and } J < 0, \tag{1.14}$$

$$DI < 0 \text{ and } J > 0, \tag{1.15}$$

or

$$DI > 0 \text{ and } J < 0. \tag{1.16}$$

Inequalities

$$DI > 0 \text{ and } J > 0 \tag{1.17}$$

characterize an imaginary cone apex. Finally, conditions

$$DI = 0 \text{ and } J < 0 \tag{1.18}$$

are related to a planar interphase boundary oriented parallel to the ZNSP. Conditions (1.14)–(1.18) are written in terms of invariants I, D, and J from (1.13). The conical interphase boundaries that obey conditions (1.14), (1.15), or (1.16) can provide a partial stress relief because of $D \neq 0$ while the planar boundaries parallel to the ZNSPs provide the complete stress relief in the heterophase state. We note that conditions (1.18) are written in the more strict form as compared to conditions (1.5) and (1.6) from the Metrat's algorithm. In the case of fulfilment of conditions (1.17), some rearrangement of the DS in the FE phase can take place to promote the further stress relief in the SC sample.

It should be mentioned that conditions (1.14)–(1.18) were first applied [77] for description of various interphase boundaries observed in $PbZrO_3$ at the FE phase transition. A possible way of the evolution of the heterophase structure in $PbZrO_3$

SCs can be concerned with the formation of a large number of nuclei in the form of wedges or prisms and with the further interaction of these nuclei [77]. An interaction between the nuclei of the new phase, especially in a relatively narrow temperature range (as observed in $PbZrO_3$ SC below $T = T_C$), represents an independent problem in kinetics of structural phase transitions. This interaction leads to the formation of the heavily twinned phases, and their physical properties can be affected by this interaction.

Results of the crystallographic description of the interphase boundaries in $PbZrO_3$ SCs [77] are represented in the diagram that links volume fractions of the 71° (109°) domain types in the FE rhombohedral phase. The diagram contains a curve that corresponds to ZNSPs in a restricted volume-fraction range; however, these ZNSPs were not predicted on the basis of the necessary conditions formulated in papers [30, 31]. Generally speaking, the presence of the ZNSP at the cubic–rhombohedral phase transition is caused by the commensurability [77] of the diagonal and off-diagonal components of the spontaneous strains in the polydomain phase of $PbZrO_3$. This circumstance is to be taken into account when formulating the necessary conditions [30, 31] for the existence of ZNSPs in heterophase and heavily twinned SCs. Hereby it is assumed that these SCs undergo the structural phase transitions between low-symmetry phases wherein the unit-cell shear strain may play an important role in the balance of the strains that influence elastic matching of the phases or domain regions.

The crystallographic concept [77] was applied for description of a system of the interphase boundaries at the electric-field-induced cubic–rhombohedral phase transition in plate-like PMN SCs [62]. The role of the mechanical stress field at the monoclinic–orthorhombic phase transition in Pb_2CoWO_6 SCs [61] was also studied on the basis of the concept from work [77]. A correlation between the value of invariant D from (1.13) and the volume density of elastic energy was first revealed at description of the heterophase Pb_2CoWO_6 SCs [61]. It should be added that jumps in the unit-cell parameters at the monoclinic–orthorhombic phase transition in Pb_2CoWO_6 SC [78] do not promote the complete stress relief in the heterophase system. As a consequence, the conical interphase boundaries in this SC would appear in the presence of the internal stress. An additional possibility for the stress relief may be concerned with the formation of transition regions that are characterized by variations of the unit-cell parameters of Pb_2CoWO_6 [61]. A detailed crystallographic description of the transition region in FE solid solutions is proposed in Sect. 5.3.

1.3 Polydomain/Heterophase Ferroelectrics

In Chap. 1 we considered various examples of interfaces in SCs of FEs and related materials. The interfaces, such as domain walls, domain boundaries, interphase boundaries, etc., are one of the factors that actively influence physical properties of heterogeneous materials. Knowledge of the interfaces and their characteristics

promotes the successful study of the physical properties, structural phase transitions, and interrelations in the fundamental triangle 'composition–structure–properties'.

Among the problems concerning the interfaces in heterogeneous FEs (including FE solid solutions), of particular interest are

1. Determination of the orientation of the domain and interphase boundaries in heavily twinned FE SCs
2. Study of correlations between the DS and interphase boundary in the context of the unit-cell behaviour at the structural phase transition (polymorphic, morphotropic, or field induced)
3. Analysis of conditions for the complete (or partial) stress relief in polydomain/heterophase FE SCs
4. Application of crystallographic methods for interpretation of experimental results on the rearrangement of the DS at the phase transitions, and
5. Study of the role of heterophase states and alternative stress-relief ways in FE solid solutions near the MPB

The aforementioned and related problems will be considered in the next chapters of the present book.

References

1. Lines M and Glass A, *Principles and Application of Ferroelectrics and Related Materials*. (Clarendon Press, Oxford, 1977)
2. Zheludev IS, *Physics of Crystalline Dielectrics. Vol. 2: Electrical Properties*. (Plenum, New York, 1971)
3. Smolensky GA, Bokov VA, Isupov VA, Krainik NN, Pasynkov RE, Sokolov AI, Yushin NK, *Physics of Ferroelectric Phenomena*. (Nauka, Leningrad (in Russian), 1985)
4. Xu Y, *Ferroelectric Materials and Their Applications*. (North-Holland, Amsterdam, London, New York, Toronto, 1991)
5. Fang D-N, Soh AK, Li C-Q, Jiang B, Nonlinear behavior of 0–3 type ferroelectric composites with polymer matrices. J. Mater. Sci. **36** 5281–5288 (2001)
6. Malbec A, Liu T, and Lynch, Characterization and modeling of domain engineered relaxor ferroelectric single crystals. J. de Phys. IV (France) **115**, 59–66 (2004)
7. Turik AV, Elastic, piezoelectric, and dielectric properties of single crystals of $BaTiO_3$ with a laminar domain structure. Sov. Phys. Solid State **12**, 688–693 (1970)
8. Topolov VYu, Bondarenko EI, Turik AV, Chernobabov AI, The effect of domain structure on electromechanical properties of $PbTiO_3$-based ferroelectrics. Ferroelectrics **140**, 175–181 (1993)
9. Topolov VYu, Interfaces in ferroelectrics and related materials with complex domain structures. Ferroelectrics **222**:41–52 (1999)
10. Topolov VYu, Bowen CR, *Electromechanical Properties in Composites Based on Ferroelectrics*. (Springer, London, 2009)
11. Fesenko EG, Gavrilyachenko VG, Semenchev AF, (1990) *Domain Structure of Multiaxial Ferroelectric Crystals*. (Rostov University Press, Rostov-on-Don (in Russian), 1990)
12. Rudyak VM, *Switching Processes in Nonlinear Crystals*. (Nauka, Moscow (in Russian), 1986)
13. Shuvalov LA, Urusovskaya AA, Zheludev IS, Zalessky AV, Semiletov SA, Grechishnikov BN, Chistyakov IG, Pikin SA, *Modern Crystallography*. Vol. 4. (Nauka, Moscow (in Russian), 1981)

14. Zheludev IS, Shuvalov LA, Ferroelectric phase transitions and symmetry of crystals. Kristallografiya **1**:681–688, (1956) (in Russian)
15. Zheludev IS, Shuvalov LA, Orientation of domains and macrosymmetry of properties of ferroelectric single crystals. Izvestiya Akademii Nauk SSSR. Seriya Fizicheskaya **21**:264–274 (1957) (in Russian)
16. Shuvalov LA, Crystallographic classification of ferroelectrics. Ferroelectric phase transitions and features of the domain structure and some physical properties of ferroelectrics of different classification species. Kristallografiya **8**:617–624 (1963) (in Russian)
17. Shuvalov LA, Crystallophysical classification of ferroelectrics and its applications. Izvestiya Akademii Nauk SSSR. Seriya Fizicheskaya **28**:660–665 (1964) (in Russian)
18. Shuvalov LA, Symmetry aspects of ferroelectricity. J. Phys. Sol. Jpn. **28** (Suppl.):38–51 (1970)
19. Zheludev IS, *Ferroelectricity and Symmetry*. In: Solid State Physics: Advances in Research and Applications. Vol. 26. (Academic, New York, London, 1971) pp 429–464
20. Mitsui T, Furuichi J, Domain structure of Rochelle salt and KH_2PO_4. Phys. Rev. **90**:193–202, (1953)
21. Cao W, Cross LE, Theory of tetragonal twin structures in ferroelectric perovskites with a first-order phase transition. Phys. Rev. **B44**:5–12 (1991)
22. Cao W, Defect stabilized periodic amplitude modulations in ferroelectrics. Phase Trans. **55**:69–78 (1995)
23. Nambu S, Sagala DA, Domain formation and elastic long-range interaction in ferroelectric perovskites. Phys. Rev. B **50**:5838–5847 (1994)
24. Rosakis P, Jiang Q, On the morphology of ferroelectric domains. Int. J. Eng. Sci **33**:1–12 (1995)
25. Dec J, *Orientacija i kinetyka granic fazowych w monokryształach* $PbTiO_3$, $NaNbO_3$ *i* $PbZrO_3$. (Universytet Śląski, Katowice (in Polish), 1990)
26. Roytburd AL, Elastic domains and polydomain phases in solids. Phase Trans. **45**:1–33 (1993)
27. Topolov VYu, Turik AV, Crystallographic aspects of interfaces in ferroelectrics. Defect Diffus. Forum **Pt A 123–124**:31–50 (1995)
28. Roitburd AL, The theory of the formation of a heterophase structure in phase transformations in solids. Sov. Phys. Uspehi **17**:326–344 (1974)
29. Roitburd AL, On the thermodynamics of martensite nucleation. Mater. Sci. Eng. A **127**:229–238 (1990)
30. Wechsler MS, Lieberman DS, Read TA, On the theory of the formation of martensite. Trans. AIME J. Metals **197**:1503–1515 (1953)
31. Lieberman DS, Wechsler MS, Read TA, Cubic to orthorhombic diffusionless phase change – experimental and theoretical studies of AuCd. J. Appl. Phys. **26**:473–484 (1955)
32. Bilby BA, Christian JW, *Martensistic Transformations*. In: The Mechanism of Phase Transformations in Metals. (The Institute of Metals, London, 1956), pp. 121–172
33. Larché FC, Coherent phase transformations. Annu. Rev. Mater. Sci. **20**:83–99 (1990)
34. Boulesteix C, Yangui B, Ben Salem M, Manolikas C, Amelinckx S, The orientation of interfaces between a prototype phase and its ferroelastic derivatives: Theoretical and experimental study. J. de Phys. (France) **47**:461–471 (1986)
35. Kato M, Shibata-Yanagisawa M, Infinitesimal deformation approach of the phenomenological crystallographic theory of martensitic transformations. J. Mater. Sci. **25**:194–202 (1990)
36. Dudnik EF, Shuvalov LA, Domain structure and phase boundaries in ferroelastics. Ferroelectrics **98**:207–214 (1989)
37. Fousek J, Janovec V, The orientation of domain walls in twinned ferroelectric crystals. J. Appl. Phys. **40**:135–142 (1969)
38. Fousek J, Permissible domain walls in ferroelectric species. Czech. J. Phys. B **21**:955–968 (1971)
39. Janovec V, A symmetry approach to domain structures. Ferroelectrics **12**:43–53 (1976)
40. Sapriel J, Domain-wall orientations in ferroelastics. Phys. Rev. B **12**:5128–5140 (1975)
41. Vagin SV, Dudnik EF, Method of interpreting the domain structure of ferroelastics. Bull. Acad. Sci. U.S.S.R. Phys. Ser. **47**(3):78–81 (1983)

42. Shuvalov LA, Dudnik EF, Pozdeyev VG, Forbidden domain boundaries in ferroelastics. Izvestiya Akademii Nauk SSSR. Seriya Fizicheskaya **51**:2119–2123 (1987) (in Russian)
43. Boulesteix C, A survey of domains and domain walls generated by crystallographic phase transitions causing a change of lattice. Physica Status Solidi (a) **86**:11–42 (1984)
44. Barkley JR, Jeitschko W, Antiphase boundaries and their interactions with domain walls in ferroelastic-ferroelectric $Gd_2(MoO_4)_3$. J. Appl. Phys. **44**:938–944 (1973)
45. Capelle B, Malgrande C, *Antiphase Domain Walls in Ferroelectric-Ferroelastic GDMO Crystals*. In: Applications of X-Ray Topographic Methods to Materials Science: Proceedings of France–U.S.A. Seminar, Village, Colo., 7–10 August 1983. (New York London, 1984) pp 511–522
46. Rychetsky I, Schranz W, Antiphase boundaries in Hg_2Br_2 and KSCN. J. Phys. Condens. Matter **5**:1455–1472 (1993)
47. Salje EKH, *Phase Transitions in Ferroelastic and Co-Elastic Crystals*. (Cambridge University Press, Cambridge, New York, Oakleigh, 1990)
48. Heine V, Bratkovsky AM, Salje EKH, The effect of clamped and free boundaries on long range strain coupling in structural phase transitions. Phase Trans. **52**:85–93 (1994)
49. Wruck B, Salje EKH, Zhang M, Abraham T, Bismayer U, On the thickness of feroelastic twin walls in lead phosphate $Pb_3(PO_4)_2$: an X-ray diffraction study. Phase Trans. **48**:135–148 (1994)
50. Bratkovsky AM, Salje EKH, Heine V, Overwiew of the origin of tweed texture. Phase Trans. **52**:77–83 (1994)
51. Putnis A, Salje E, Tweed microstructures: Experimental observations and some theoretical models. Phase Trans. **48**:85–105 (1994)
52. Bratkovsky AM, Marais SC, Heine V, Salje EKH, The theory of fluctuations and texture embryos in structural phase transitions mediated by strain. J. Phys. Condens. Matter **6**:3679–3696 (1994)
53. Viehland D, Li JF, Colla EV, Domain structure changes in $(1 - x)Pb(Mg_{1/3}Nb_{2/3})O_3 - xPbTiO_3$ with composition, dc bias, and ac field. J. Appl. Phys. **96**:3379–3381 (2004)
54. Noheda B, Structure and high-piezoelectricity in lead oxide solid solutions. Curr. Opin. Solid State Mater. Sci. **6**:27–34 (2002)
55. Bokov AA, Ye Z-G, Domain structure in the monoclinic *Pm* phase of $Pb(Mg_{1/3}Nb_{2/3})O_3 - PbTiO_3$ single crystals. J. Appl. Phys. **95**:6347–6359 (2004)
56. Shuvaeva VA, Glazer AM, Zekria D, The macroscopic symmetry of $Pb(Mg_{1/3}Nb_{2/3})_{1-x}Ti_xO_3$ in the morphotropic phase boundary region ($x = 0.25 - 0.5$). J. Phys. Condens. Matter **17**:5709–5723 (2005)
57. Bokov AA, Ye Z-G, Recent progress in relaxor ferroelectrics with perovskite structure. J. Mater. Sci. **41**:31–52 (2006)
58. Topolov VYu, Turik AV, Elastic interaction of phases of $Gd_2(MoO_4)_3$ crystals. Izvestiya Vysshikh Uchebnykh Zavedeniy, Fizika **33**(3): 68–72 (1990) (in Russian)
59. Nakamura T, Kondo T, Kumada A, Observation of phase boundaries between ferro- and paraelectric phases in $Gd_2(MoO_4)_3$ crystals. Solid State Commun. **9**:2265–2268 (1971)
60. Metrat G, Theoretical determination of domain structure at transition from twinned phase: application to the tetragonal-orthorhombic transition of $KNbO_3$. Ferroelectrics **26**:801–804 (1980)
61. Topolov VYu, Rabe H, Schmid H, Mechanical stresses and transition regions in polydomain Pb_2CoWO_6 crystals. Ferroelectrics **146**:113–121 (1993)
62. Topolov VYu, Ye Z-G, Schmid H, A crystallographic analysis of macrodomain structure in $Pb(Mg_{1/3}Nb_{2/3})O_3$. J. Phys. Condens. Matter **7**:3041–3049 (1995)
63. Topolov VYu, Ye Z-G, Formation of the stress-induced *mm*2 phase at the ferroelastic – antiferroelectric $\bar{4}3m - \bar{4}2m$ phase transition in Cr − Cl boracite. J. Phys. Condens. Matter **8**:6087–6094 (1996)
64. Topolov VYu, Peculiarities of coexistence of heavily twinned phases in the $(1 - x)Pb(Mg_{1/3}Nb_{2/3})TiO_3 - xPbTiO_3$ solid solutions at $0.23 \leq x \leq 0.30$. Crystallogr. Reports **52**:297–301 (2007)

65. Balyunis LE, Topolov VYu, Bah IS, Turik AV, The S-type domain and twin boundaries in plate-like $PbZrO_3$ crystals having complicated twinned structures. J. Phys. Condens. Matter **5**:1419–1426 (1993)
66. Topolov VYu, Balyunis LE, Turik AV, Eremkin VV, Sori BI, S-type twinning (domain) boundaries in $PbZrO_3$ crystals. Sov. Phys. Crystallogr. **37**:223–226 (1992)
67. Topolov VYu, *On Variety of Conditions for Realization of S-type Domain Boundaries in Ferroelectric Crystals*. In: Proceedings of the All-Union Conference "Real Structure and Properties of Acentric Crystals", September 17–22, 1990, Aleksandrov, VNIISIMS. Pt 2. Blagoveshchensk, (1990) pp 20–29 (in Russian)
68. Topolov VYu, Gagarina ES, Demidova VV, Domain structure and related phenomena in $PbYb_{0.5}Nb_{0.5}O_3$ crystals. Ferroelectrics **172**:373–376 (1995)
69. Balyunis LE, Topolov VYu, Turik AV, Fesenko OE, Optical and crystallographic studies of twin and phase boundaries in antiferroelectric $PbHfO_3$. Ferroelectrics **111**:291–298 (1990)
70. Topolov VYu, Turik AV, Fesenko OE, Eremkin VV, Mechanical stresses and three-phase states in perovskite-type ferroelectrics. Ferroelectrics Lett. Sect. **20**:19–26 (1995)
71. Topolov VYu, Electromechanical Interactions in Heterogeneous Systems at Ferroelectric Phase Transitions. Author's Abstract to the Thesis, Cand. Sci. (Phys. & Math.). Rostov State University, Rostov-on-Don, (1987) (in Russian)
72. Topolov VYu, Analysis of conditions necessary for the existence of a flat non-deformed boundary separating polydomain ferroelastic phases. Bulletin of the Academy of Sciences of the USSR. Phys. Ser. **53** (7), 51–54 (1989)
73. Kuhn W, Domain structures induced by phase transitions in $BaTiO_3$ single crystals. Ferroelectrics Lett. Sect. **13**:101–108 (1991)
74. Topolov VYu, Some features of three-phase states in $PbZr_{1-x}Ti_xO_3$ crystals. Crystallogr. Reports **43**, 68–73 (1998)
75. Lekhnitsky SG, *Elasticity Theory of the Anisotropic Solid*. (Nauka, Moscow, 1977) (in Russian)
76. Mura T, *Micromechanics of Defects in Solids*. (Martins Nijhoff Publications, Dordrecht, 1987)
77. Topolov VYu, Balyunis LE, Turik AV, Bah IS, Fesenko OE, Interphase boundaries at cubic-rhombohedral phase transition in $PbZrO_3$ crystals. Bulletin of the Russian Academy of Sciences. Physics **56**:1588–1593 (1992)
78. Sciau Ph, Calvarin G, Sun BN, Schmid H, X-ray study of phase transitions of the elpasolite-like ordered perovskite Pb_2CoWO_6. Physica Status Solidi (a) **129**:309–321 (1992)
79. Ye Z-G, Topolov VYu, Complex domain and heterophase structures in $Pb(Mg_{1/3}Nb_{2/3})O_3$ – $PbTiO_3$ single crystals. Ferroelectrics 253:79–86 (2001)

http://www.springer.com/978-3-642-22482-9

Heterogeneous Ferroelectric Solid Solutions
Phases and Domain States
Topolov, V.Y.
2012, XIV, 158 p., Hardcover
ISBN: 978-3-642-22482-9